Enhanced far-infrared absorption in $CePd_3$ and $YbCuSi_2$. Experiment

F. E. Pinkerton* and A. J. Sievers
Laboratory of Atomic and Solid State Physics and Materials Science Center, Cornell University, Ithaca, New York 14853

M. B. Maple and B. C. Sales†
Institute for Pure and Applied Physical Sciences, University of California, San Diego, La Jolla, California 92093
(Received 15 August 1983)

Experimental results are presented for far-infrared optical measurements on the valence fluctuation compounds $CePd_3$, $YbCu_2Si_2$, $CeAl_3$, $CeCu_2Si_2$, and YbCuAl at photon energies between 3 and 40 meV and temperatures between 4.2 and 150 K. The optical absorptivities of the valence-fluctuation compounds were measured using a dual-cavity technique. An improved analysis of the dual-cavity technique was developed so that an absolute measurement of the sample absorptivity could be extracted from the data. The absorptivities of $CePd_3$ and $YbCu_2Si_2$ at helium temperature show a broad anomaly near 20 meV. No such feature is seen in the isostructural integral valent-analog compounds YPd_3, $DyPd_3$, or $LuCu_2Si_2$. The absorptivity is also strongly temperature dependent, decreasing in magnitude with increasing temperature up to 150 K, where the absorptivity has a Drude-type frequency dependence. The anomaly in $CePd_3$ is virtually independent of whether the optical surface is prepared by mechanical polishing or by chemical etching. $CePd_3$ also has sharp absorption features at 14.7 and 21.6 meV. Their positions and widths are independent of temperature and applied magnetic field although the magnitude of the feature decreases with increasing temperature, vanishing by 150 K. Both of these features have been identified with $q=0$ optic phonons. No anomalies have been seen in the absorptivities of $CeAl_3$, $CeCu_2Si_2$, or YbCuAl between 3 and 40 meV. The characteristic energies of anomalies in other physical properties of these compounds, however, are an order of magnitude smaller than those in $CePd_3$ and $YbCu_2Si_2$, so that the absence of a resonance above 3 meV in the former compounds is to be expected.

I. INTRODUCTION

Among the rare-earth (RE) compounds, the "valence-fluctuation" (VF) or "intermediate-valence" metals form a special subset characterized by a nonintegral occupation number of the RE $4f$ subshell.[1–8] The near degeneracy of the $4f^n$ and $4f^{n-1}5d$ rare-earth electronic configurations (or valences) allow an electron to transfer back and forth between the $4f$ subshell and the $5d$ conduction band at the Fermi level. The coexistence of localized $4f$ states with the delocalized conduction-electron states manifests itself through anomalous behavior in a wide variety of physical properties,[2,3] but the crucial experimental hallmarks of VF materials are as follows: (1) A superposition of the signatures of the two configurations in x-ray absorption and x-ray photoemission spectroscopy (XPS), (2) a weighted average in the Mössbauer isomer shift and static measurements such as lattice constant, and (3) a transition in the magnetic susceptibility from a high-temperature magnetic regime to a low-temperature "nonmagnetic" regime, which neither orders magnetically nor shows a Curie divergence. This transition typically occurs at thermal energies in the neighborhood of 1—10 meV and is often accompanied by anomalies in the temperature dependence of the transport properties.

The present work centers on the VF compounds $CePd_3$ and $YbCu_2Si_2$, containing rare-earth elements from either end of the RE series. The evidence for VF behavior in these two materials rests mainly on lattice constant and susceptibility data. In $CePd_3$, for example, a simple interpolation of the measured lattice constant between those predicted on the basis of the ionic radius of the Ce^{3+} ($4f^1$) and Ce^{4+} ($4f^0 5d$) configurations gives 3.4 as an estimate of the average Ce valence.[9] Similarly, the lattice constant of $YbCu_2Si_2$ departs from the trend established by the rest of the $\mathscr{R}Cu_2Si_2$ series,[10] implying a mixture of the Yb^{2+} ($4f^{14}$) and Yb^{3+} ($4f^{13}5d$) valences. The crossover between magnetic and nonmagnetic susceptibility occurs at a thermal energy kT of roughly 20 meV in both materials.[9,11] Both materials also have anomalies in the temperature dependence of the electrical resistivity at about the same energy.[10,12] These experiments demonstrate the relevance of *low* energies (~ 10 meV) in VF materials.

The spectra of VF materials can be roughly divided into two energy regimes, the high-energy (greater than 0.1 eV) interband regime and the low-energy (less than 0.1 eV) intraband regime. The vast majority of optical measurements on VF compounds have concentrated on the high-energy regime.[13–29] At these energies it is possible in principle to observe directly the interband excitations of the two configurations, just as in XPS. In fact, a few weak interband transitions have been observed, for example, in TmSe above 2 eV.[28] Below 2 eV, however, the rapid rise to high reflectivity below the conduction-electron plasma edge masks the weak interband response. Most

studies, therefore, have focused on the energy of the plasma edge as a measure of the number of conduction electrons, and hence the effective RE valence. The plasma edge in CeN, for example,[24] gives an estimated contribution of 0.4 electrons from the Ce f shell, or an effective valence of 3.4, in agreement with the valence estimated from the lattice constant.

In view of the importance of the 10-meV-energy regime, there have been surprisingly few studies of the low-energy electronic intraband spectrum with the use of optical spectroscopy. This is doubtless largely due to the experimentally formidable task of making accurate quantitative reflectivity measurements in the far infrared (FIR), where the reflectivity of metals is nearly 1. Furthermore, at room temperature the thermal energy kT is larger than the photon energies. Reducing the temperature to remove thermal effects adds the further complication of carrying out the optical measurements under cryogenic conditions. Prior to the work presented here, the reflectivity of $CePd_3$ had been measured only at room temperature. Allen *et al.* did not report any FIR anomalies down to 5 meV.[29] Recently, however, Hillebrands *et al.* have observed a small deviation from simple metallic behavior near 20 meV.[30] Other studies have been carried out on the VF compounds SmB_6 and TmSe. Allen *et al.*[31] have investigated the reflectivity of SmB_6 at room temperature down to 20 meV and found evidence, supported by resistivity measurements, that SmB_6 is nonmetallic at low energies. Batlogg *et al.* have extended these measurements down to 2 meV on SmB_6 thin films at 4 K and also report evidence for a deep minimum in the density of states at the Fermi level.[32] One study of TmSe at 4 K found no anomalies in the FIR optical properties,[33] but recent work has revealed a deviation from Drude behavior at room temperature and 77 K in the intraband regime.[28] Both SmB_6 and TmSe, however, are qualitatively different from the Ce and Yb VF intermetallics, as will be discussed later.

The concurrence of phonon frequencies with the low-energy electronic intraband regime has attracted Raman scattering studies of the phonon spectra in VF materials.[34–37] Most of the spectral weight in these Raman experiments lies in the phonons at the Brillouin-zone boundary. In the VF system SmS, for example, softening of the optic phonons at the zone boundary has been observed,[35] which is consistent with a softening of the phonon dispersion curves seen in neutron scattering results on the alloy system $Sm_{1-x}Y_xS$ ("chemically collapsed SmS"). A similar softening has been seen in the optic phonons of Tm_xSe.[37]

This paper expands on our discovery of anomalies in the low-temperature FIR optical response of $CePd_3$ and $YbCu_2Si_2$ VF compounds, which we reported in earlier publications.[38,39] Section II outlines our extension of a known FIR technique to measure quantitatively the reflectivity of samples at cryogenic temperatures. Our optical results for VF materials are presented in Sec. III; they show a broad absorption enhancement in $CePd_3$ and $YbCu_2Si_2$ at low temperature and, additionally, optic phonon excitations in $CePd_3$. Section IV gives some concluding remarks.

II. EXPERIMENTAL

A. Sample preparation

Polycrystalline samples of $\mathscr{R}Pd_3$ ($\mathscr{R}$=Y,Ce,Dy), $\mathscr{R}Cu_2Si_2$ ($\mathscr{R}$=Ce,Yb,Lu), $CeAl_3$, and YbCuAl (Ref. 40) were prepared by arc melting in an argon atmosphere. The samples were annealed as shown in Table I, and all samples consisted of a single phase according to x-ray diffraction analysis. The crystal structures and lattice constants are also listed in Table I. Two samples of $CePd_3$ were investigated, denoted here as $CePd_3$(a) and $CePd_3$(b).[41] X-ray diffraction analysis indicated that the samples of $CePd_3$ did not require annealing, and so most of the optical measurements were done on unannealed samples. Nevertheless, one sample $CePd_3$(a) was investigated prior to and after annealing to confirm that annealing had no significant effect on the low-energy optical

TABLE I. Crystal structure and annealing procedure for the samples used in this work.

Sample	Symmetry	Structure	a (Å)	c (Å)	Anneal time (weeks)	Temperature (°C)
$CePd_3$(a)[a]	cubic	Cu_3Au	4.120		Not annealed	
$CePd_3$(a)					1	700
$CePd_3$(b)					Not annealed	
$DyPd_3$[a]	cubic	Cu_3Au	4.061		1	850
YPd_3[b]	cubic	Cu_3Au	4.062		1	850
$CeCu_2Si_2$[c]	tetragonal	$ThCr_2Si_2$	4.105	9.933	1	800
$YbCu_2Si_2$[c]	tetragonal	$ThCr_2Si_2$	3.926	9.987	1	800
$LuCu_2Si_2$[c]	tetragonal	$ThCr_2Si_2$	3.907	10.004	1	800
$CeAl_3$[d]	hexagonal	Ni_3Sn	6.545	4.609	4	900
YbCuAl[e]	hexagonal	Fe_2P	6.925	3.984	1	830

[a]Reference 9.
[b]Reference 63.
[c]Reference 64.
[d]Reference 65.
[e]Reference 66.

spectrum. All $CePd_3$ results are for unannealed samples unless otherwise specified.

Slices about 0.5 mm thick and about 1 cm in diameter were cut from the ingot and mechanically polished to 1-μm grit size. The optical measurements were then carried out on these mechanically prepared surfaces. The optical results were shown to be relatively insensitive to the method of surface preparation by testing a second technique on $CePd_3$(a), in which polished slices were subsequently immersed for 3 min in an agitated acid etch (75 vol% HCl and 25 vol% HNO_3 diluted 50%). The etch removed the polished surface layer, and visual examination could clearly distinguish the individual grains.

B. Connection between the absorptivity and the dielectric function

While a viable technique for measuring the optical properties of metals in the visible,[42] a simple reflection experiment lacks sensitivity in the far-infrared intraband regime, where the reflectivity R of metals is very high (typically 95% or better). The absorptivity $A=1-R$ at normal incidence provides a much more sensitive measure of the optical response. The absorptivity of a surface is simply the fraction of incident power absorbed on a single reflection. In general it depends not only on the frequency ω of the incident radiation, but also on the angle of incidence. For the case of normal incidence,[43]

$$A \simeq 4r \ , \tag{1}$$

where r is the real part of the reduced surface impedance[43]

$$z(\omega)=r+ix=[\mu(\omega)/\epsilon(\omega)]^{1/2} \ . \tag{2}$$

Here $\epsilon(\omega)$ and $\mu(\omega)$ are the dielectric function and the magnetic permeability, respectively. For nonmagnetic metals $\mu(\omega)\simeq 1$, and we will neglect it henceforth. In turn $\epsilon(\omega)$ is related to the ac conductivity $\sigma(\omega)$ by[44]

$$\epsilon(\omega)=1+\frac{4\pi i\sigma(\omega)}{\omega} \ . \tag{3}$$

The complex surface impedance $z(\omega)$, dielectric function $\epsilon(\omega)$, or conductivity $\sigma(\omega)$ provide equivalent descriptions of the dielectric response of the material.

A free-electron metal can be modeled by the Drude theory,[44] in which the scattering of conduction electrons is parametrized by a frequency-independent relaxation time τ. The ac conductivity is then[44]

$$\sigma(\omega)=\frac{\sigma_0}{1-i\omega\tau}, \quad \sigma_0=\frac{\omega_p^2\tau}{4\pi} \ , \tag{4}$$

where σ_0 is the dc electrical conductivity and ω_p is the plasma frequency. In the far-infrared limit $\omega\tau \ll 1$ the corresponding surface impedance is

$$z(\omega)=\left[\frac{\omega}{8\pi\sigma_0}\right]^{1/2}(1-i) \ . \tag{5}$$

Note that $x/r=-1$ for a Drude metal in the limit where $\omega\tau \ll 1$. The far-infrared absorptivity has the particularly simple Hagen-Rubens form

$$A(\omega)=\left[\frac{2\omega}{\pi\sigma_0}\right]^{1/2} \ , \tag{6}$$

in which A increases as $\omega^{1/2}$ with a magnitude scaled by the dc conductivity σ_0.

C. The dual-cavity technique

We measure the absorptivity of the bulk samples, using a dual nonresonant cavity technique.[45] By "nonresonant" we mean that the wavelengths of interest are much smaller than any of the dimensions of the cavity, so that there are no preferred resonant modes, but rather a large number of closely spaced and nearly equally excited modes. The radiation in the cavity can then be thought of as a uniformly distributed photon gas.[46] The radiation is coupled by a light cone through a small hole into a brass cavity partially lined with sample. The geometry of the light cone is such that the light is spread through 2π solid angle as it passes out of the cone and into the cavity, so that the hole effectivity resembles a point source. After about 100 reflections on average the light exits either back through the entrance hole or through a second small hole leading to the detector. A second cavity consisting entirely of brass serves as a reference. The details of the experimental technique have been given elsewhere.[47] An abbreviated discussion follows.

The use of nonresonant single cavities in the far infrared was pioneered by Richards and Tinkham,[46] and subsequently used by a number of investigators to study the energy gap in superconductors.[48–50] Dual cavities have also been used as a qualitative measure of sample absorptivity.[51–53] We have refined an approximate analysis of microwave cavities by Lamb[54] and extended it to the dual-cavity technique to extract absolute quantitative values for the absorptivity from the dual-cavity measurements.

Broadband radiation from a mercury arc lamp is chopped at low frequency (50–100 Hz) and passes through a step-and-integrate Michelson interferometer[55] for the frequency analysis. This signal beam is directed by a $\frac{1}{2}$-in diameter light pipe into a cryostat containing liquid ^{4}He at 4 K. After passing through the sample chamber containing the cavities, the radiation is filtered by cold alkali halide filters and/or black polyethylene, then detected by a Ge bolometer cooled to 0.3 K with the use of a closed liquid-^{3}He system pumped by a charcoal pot.[56] The chopped signal beam is phase-sensitive detected by a lock-in amplifier. The maximum frequency available is set by a sapphire window at the detector, which is opaque at frequencies above 350 cm^{-1} (43 meV). The lower frequency limit is set by the breakdown of the nonresonant condition at frequencies below about 30 cm^{-1} (4 meV).

With the reference cavity in the signal beam, the intensity $I_r(\omega)$ transmitted through the cavity is measured as a function of frequency ω. The sample cavity is then rotated into the beam and the transmitted intensity $I_s(\omega)$ is measured. Typically three spectra are taken at each cavity and averaged, although for high-resolution data only a

single spectrum is taken. The averaged transmission spectra of the reference and sample cavities are ratioed to obtain $I_s(\omega)/I_r(\omega)$. This ratio clearly gives a qualitative measure of the absorptivity of the sample. If, for example, the sample has a higher absorptivity than does the reference material (brass) at frequency ω, the ratio I_s/I_r will be less than 1 at that frequency. It is in this qualitative sense that the dual-cavity technique has been employed in the past. We have shown, however, that *quantitative* information can be obtained.

Within the cavity the radiation is effectively incident on the sample at all angles. To within a few percent the angle-averaged absorptivity $\bar{A}$ in the FIR (where $r\sim|x|\sim10^{-2}$) is given by[57]

$$\bar{A}=4r[\tfrac{4}{3}+c(r)]\,, \tag{7}$$

where the correction $c(r)=r[\ln(2r^2/1+2r)-\frac{1}{2}]$. Comparison of the energy transmitted through the reference and sample cavities gives

$$\frac{I_s(\omega)}{I_r(\omega)}=1-\frac{S_s(\bar{A}_s-\bar{A}_r)}{2S_h+S_s\bar{A}_s+(S-S_s)\bar{A}_r}\,, \tag{8}$$

where $\bar{A}_s$ and $\bar{A}_r$ are the angle-averaged absorptivities of the sample and reference material, respectively. The quantities S, S_s, and S_h are geometrical quantities describing the cavities, with S being the total interior surface area of each cavity, S_s being the surface area of the sample within the sample cavity, and S_h being the area of each input and ouput hole. The absorptivity at normal incidence A_s of the sample is obtained from Eqs. (1), (7), and (8) and from the measured intensity ratio I_s/I_r. The absorptivity $\bar{A}_r$ of the reference material (brass) is simply that of a Drude metal with the corresponding dc electrical conductivity.

The dependence of the sample absorptivity on magnetic fields up to 75 kG was studied using a superconducting magnet cryostat.[58] Because of the small bore of the magnet, only a single cavity could be used. This limited the magnetic experiments to comparisons of the spectra of a single sample cavity taken in different magnetic fields.

In order to connect the ac optical response with the dc transport properties, we have also investigated the temperature dependence of the electrical resistivity of all the samples. The resistivity was measured on bars cut from the ingot, using a standard four-probe low-frequency ac technique.

III. ABSORPTIVITY OF VALENCE FLUCTUATORS

In this section we present the results of dc resistivity and FIR optical-absorptivity measurements on the valence-fluctuation compounds $CePd_3$, $YbCu_2Si_2$, $CeAl_3$, $CeCu_2Si_2$, and YbCuAl, as well as related integral-valent analog compounds. Both nonmagnetic (YPd_3) and magnetic ($DyPd_3$) isostructural analogs of VF $CePd_3$ have been measured. The Y^{3+} ion in YPd_3 has the filled-shell electronic configuration of krypton and hence has no magnetic moment. YPd_3 was used instead of the rare-earth nonmagnetic analog compound $LaPd_3$ because the latter degrades in air. The Dy^{3+} ion $DyPd_3$ has a $^6G_{15/2}$ spin-orbit f-electron ground state with an effective magnetic moment of $10.6\mu_B$. $LuCu_2Si_2$ is isostructural to $YbCu_2Si_2$ and $CeCu_2Si_2$, but the Lu ion has a filled $4f$ shell and hence has no magnetic moment.

A. $CePd_3$

1. *Intraband absorptivity*

The electrical resistivity of $CePd_3$ exemplifies the anomalies seen in the transport properties of VF compounds. The dc resistivity of $CePd_3$(a) as a function of temperature is shown in Fig. 1. The resistivity rises sharply with increasing temperature up to a maximum of about 165 $\mu\Omega$ cm near 120 K ($kT=10$ meV), then decreases slowly up to room temperature. This behavior agrees with independent measurements on other samples of $CePd_3$.[12] The resistivity at 4 K can be used as a rough gauge of sample stoichiometry,[12] and the value of 41 $\mu\Omega$ cm found for our sample indicates that it is of quite satisfactory quality. By comparison the resistivities of YPd_3 and $DyPd_3$ in Fig. 1 show typical metallic behavior, characterized by a linear temperature dependence at high temperature and saturating to a residual resistivity due to disorder scattering at low temperature.

Before turning to the optical absorptivity of $CePd_3$, it is instructive to examine the absorptivity of the non-VF analog compounds YPd_3 and $DyPd_3$. The frequency-dependent absorptivity of YPd_3 at low temperature, shown in Fig. 2, does indeed show the simple Drude behavior predicted by Eq. (6). The shape and magnitude of the absorptivity agree to within the experimental error ($\pm15\%$) with the Drude response calculated from the dc resistivity at 5 K (25.6 $\mu\Omega$ cm), indicated as the dashed curve in Fig. 2. The 15% error in absorptivity is equivalent to measuring the reflectivity to an accuracy of 0.004. Furthermore, most of the error lies in assigning the *absolute magnitude* of the absorptivity, that is, in establishing the vertical scale. The error in the *shape* of the curve is substantially smaller. We also find a Drude-type frequency dependence for $DyPd_3$. The magnitude of the absorptivity is much smaller in $DyPd_3$, however, due to its

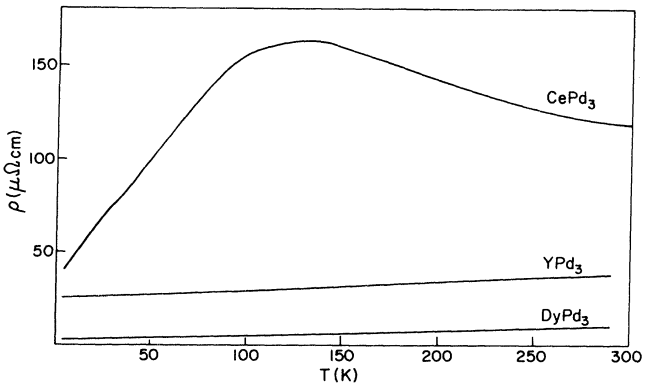

FIG. 1. Electrical resistivity of $CePd_3$ and the two isostructural compounds YPd_3 and $DyPd_3$.

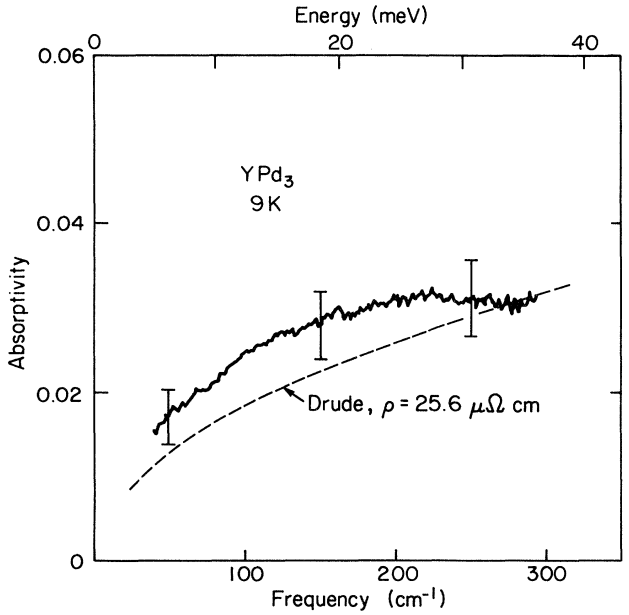

FIG. 2. Absorptivity of YPd_3 as a function of frequency at low temperature. The dashed curve gives the predicted Drude absorptivity calculated with the use of Eq. (6) and the measured dc electrical resistivity of 25.6 $\mu\Omega$ cm at 5 K. The instrumental resolution is 1.4 cm^{-1}.

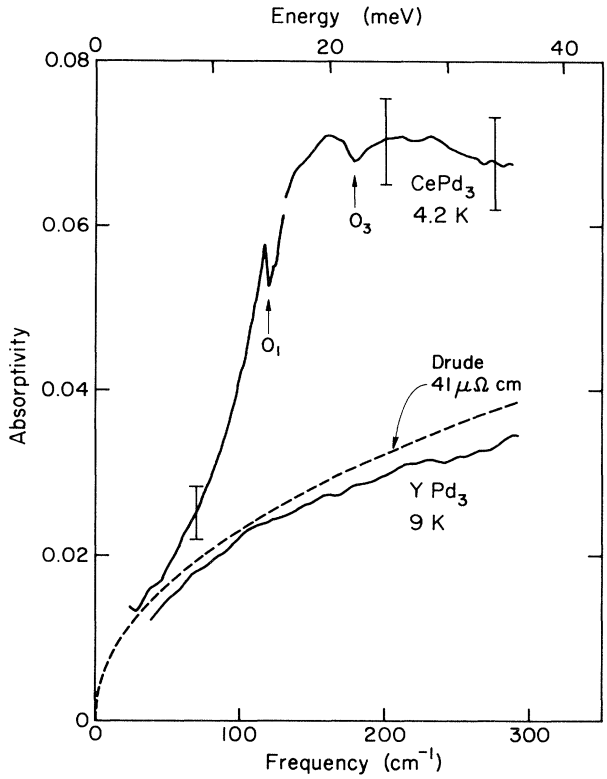

FIG. 3. Absorptivity of $CePd_3$ as a function of frequency at helium temperature. Also shown is the absorptivity of YPd_3. The dashed curve gives the predicted Drude absorptivity of $CePd_3$ calculated from its dc electrical resistivity of 41 $\mu\Omega$ cm with Eq. (6). The instrumental resolution is 8 cm^{-1} above 130 cm^{-1} and 3 cm^{-1} below 130 cm^{-1}.

much lower dc resistivity, and consequently it is much more difficult to measure accurately. The large error bars unfortunately preclude a meaningful quantitative comparison with Drude theory. Nevertheless, the absence of anomalies in the absorptivity of magnetic $DyPd_3$ demonstrates that the anomaly observed in $CePd_3$ arises from its VF character and not merely from the presence of a magnetic moment. For both YPd_3 and $DyPd_3$ the temperature dependence of the absorptivity is weak, consistent with the weak temperature dependence in the dc resistivity.

The optical absorptivity of $CePd_3$(a) at 4 K is shown as a function of frequency in Fig. 3. The dashed curve gives the predicted Drude response of $CePd_3$ at 4 K calculated from Eq. (6) with the use of the measured dc electrical resistivity of 41 $\mu\Omega$ cm. For comparison the low-temperature absorptivity of YPd_3 (at lower instrumental resolution) is also shown. The low-temperature absorptivity of $CePd_3$ departs radically from the Drude prediction with increasing frequency, reaching a peak near 150 cm^{-1} (20 meV) enhanced by about a factor of 2.5 above the Drude prediction. The deviation from Drude behavior is particularly emphasized by the region of positive curvature below 120 cm^{-1} (15 meV). Above the peak at 150 cm^{-1} the absorptivity remains roughly flat up to 290 cm^{-1} (35 meV). We have attempted to push the measurements to higher frequency, however, our spectrometer is less accurate above 300 cm^{-1}, primarily because of imperfections in the moving mirror translation stage. Figure 4 summarizes the results of four trials in the frequency region 200—500 cm^{-1}. Although the results show some spread, they indicate that the frequency response is basically flat in this region, and that the absorption anomaly

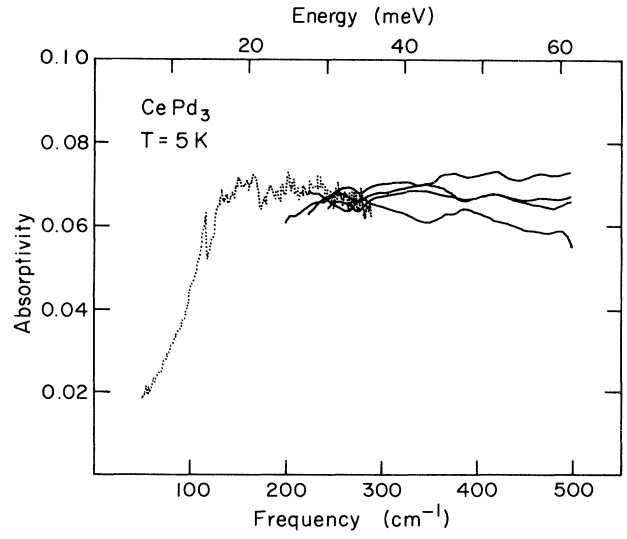

FIG. 4. Low-temperature absorptivity of $CePd_3$ extended to 500 cm^{-1}. The results of four measurements between 200—500 cm^{-1} are shown. The dotted curve is the same high-resolution (1.4-cm^{-1}) data for polished $CePd_3$ shown in Fig. 6. The instrumental resolution of the high-frequency data is 11.5 cm^{-1}.

extends at least up to 500 cm^{-1} (62 meV).

Superimposed on the main broad anomaly in Fig. 3 is a sharp secondary feature (labeled O_1) near 120 cm^{-1} (15 meV), which is not resolved in these data. A similar drop in absorptivity (labeled O_3) at about 175 cm^{-1} (22 meV) is a real, reproducible feature of the data and hints at a second sharp feature at this energy. No such features are seen in YPd_3 and $DyPd_3$, even in the high-resolution data of Fig. 2. These two sharp features are discussed in Sec. III A 2 below, where the nomenclature will become evident.

The absorptivity is strongly temperature dependent, as shown in Fig. 5. The magnitude of the broad enhancement decreases with increasing temperature, until at 150 K the absorptivity has a Drude-type behavior. The absorptivity at 150 K is roughly consistent with the room-temperature reflectivity data of Allen *et al.*[29]

In order to test the sensitivity of the results to the method of surface preparation, two more slices of $CePd_3$(a) from the same ingot were prepared by first polishing the samples as usual, then using a chemical etch to remove the polished layer. After the etch the grain boundaries in the polycrystalline samples were clearly delineated. The absorptivity of etched $CePd_3$(a) at helium temperature is shown in Fig. 6, along with the absorptivity of polished $CePd_3$(a) samples for comparison. The resolution of both curves is 1.4 cm^{-1}. The shapes of the two curves are nearly identical, agreeing to well within the error bars at low frequency, and with the etched sample lying slightly higher at high frequencies. Even at the high resolution of these curves the sharp feature O_1 at 118 cm^{-1} (14.7 meV) is not fully resolved. It is noteworthy that the sharp spike is more pronounced in the etched sample, and so is unlikely to be a surface-related feature. The improved signal-to-noise ratio of the etched sample data clearly shows the second sharp feature O_3 at 174 cm^{-1} (21.6 meV). Figure 6 demonstrates clearly that the broad anomaly in the absorptivity of $CePd_3$ is almost completely insensitive to the method of surface preparation.

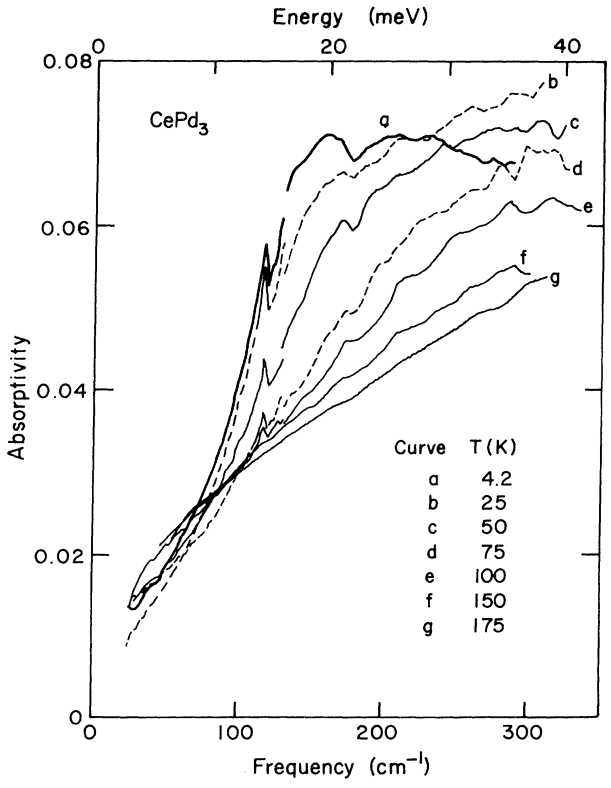

FIG. 5. Absorptivity of $CePd_3$ as a function of frequency and temperature. The instrumental resolution is 8 cm^{-1} above 130 cm^{-1} and 3 cm^{-1} below 130 cm^{-1}.

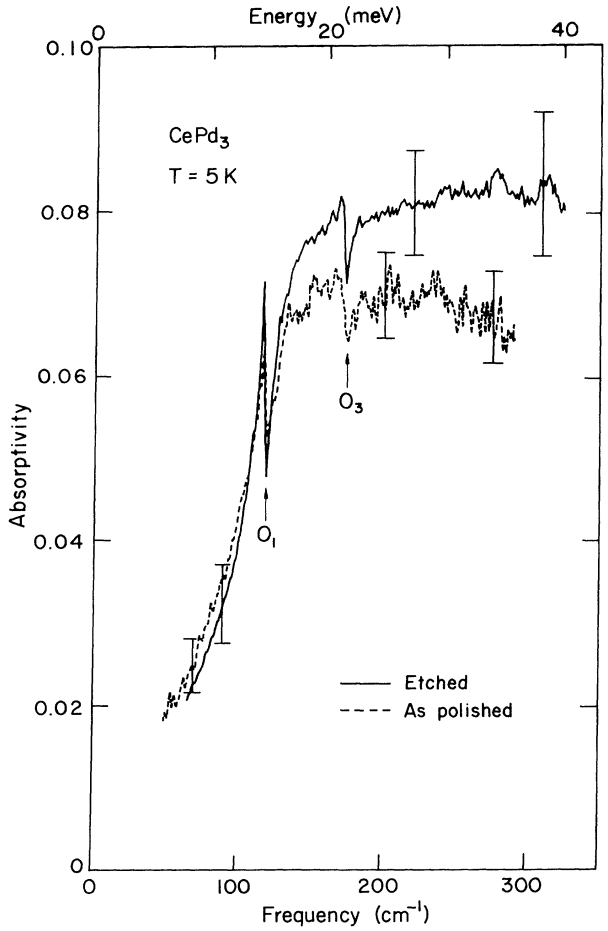

FIG. 6. Comparison of the absorptivity of etched $CePd_3$ (solid line) to that of polished $CePd_3$ (dashed line) at helium temperature. The instrumental resolution of both curves is 1.4 cm^{-1}. Note the second feature of 174 cm^{-1}.

We have also tested the effect of annealing on the absorptivity. Figure 7 shows etched $CePd_3$(a) both before and after annealing for one week at 700 °C in an evacuated quartz crucible. The annealed sample was re-etched to remove the surface contamination from residual gases in the quartz tube. As Fig. 7 shows, the absorption anomaly was essentially unchanged by annealing. The differences between the two curves can be attributed primarily to the change in the amount of disorder scattering resulting from the anneal. It has been reported that improper annealing can degrade the quality of $CePd_3$ samples.[59] We consider that the maintenance of the absorption anomaly and low residual resistivity indicate that our sample has been successfully annealed.

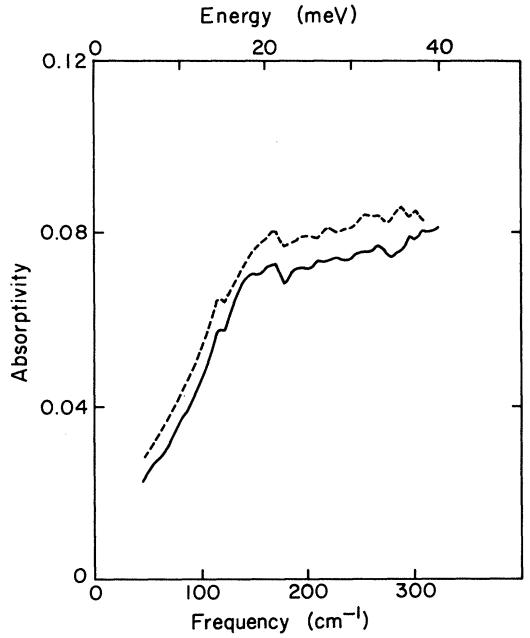

FIG. 7. Low-resolution spectra of $CePd_3$. Etched sample, dashed curve; etched and annealed sample, solid curve.

Finally, we have compared our unannealed sample $CePd_3$(a) with another unannealed sample $CePd_3$(b) prepared at another laboratory. These results are shown in Fig. 8. The two independent samples show essentially the same frequency response. The features O_1 and O_3 do not show up in these curves because of the low resolution of the data. They are present in both samples at higher resolution.

In our earlier report[39] we attributed the broad anomaly to conduction-electron scattering from a resonant level at an energy E_r away from the Fermi level and with width Γ. We described the scattering by a frequency-dependent conduction-electron relaxation time $\tau(\omega)$ given by

$$\frac{1}{\tau(\omega)}=\frac{S(\Gamma/2)^2}{(\omega-E_r)^2+(\Gamma/2)^2}\ . \tag{9}$$

This model successfully fit the data over a limited frequency range below 200 cm^{-1}. However, the oversimplification of treating the scattering by the completely real quantity $\tau(\omega)$ accounts for the model's failure above the resonant peak. In fact, the optical constants derived from this model do not necessarily obey the KK relations. A more sophisticated analysis of the complex ac conductivity due to resonant scattering fits the observed absorptivity throughout the measured frequency range. Details of this analysis will be given in a future publication.

We have evaluated the optical constants of $CePd_3$ in the far infrared by converting our absorptivity data to reflectivity $R=1-A$ and performing a standard KK analysis to obtain the phase shift θ. The data were artificially smoothed to remove the noise prior to the KK analysis. This smoothing process removed the spike O_3 at 21.6 meV, but the feature O_1 at 14.7 meV was intentionally preserved. The data were extended below 4 meV with the use of a Drude-model extrapolation. At frequencies above 40 meV the data were connected smoothly to the room-temperature data of Allen *et al.*[29] At very high frequencies (greater than 5 eV) a ν^n extrapolation was used. A number of schemes for connecting the data and extrapolating at high frequencies were tried, but the salient features of the KK results were relatively insensitive to the details of the schemes. Figures 9 and 10 show the real

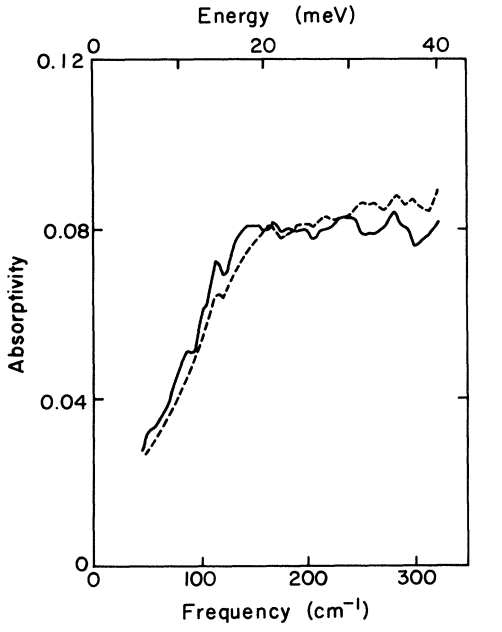

FIG. 8. Low-resolution spectra of samples from two sources. $CePd_3$(a), dashed curve; $CePd_3$(b), solid curve.

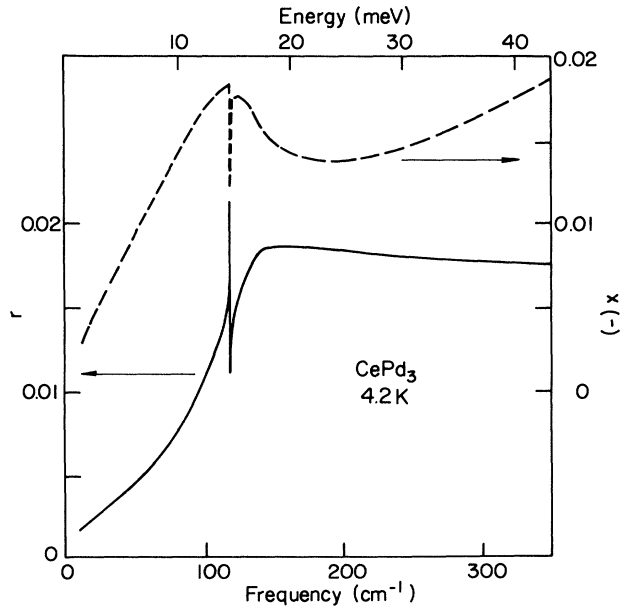

FIG. 9. Real part r (solid line) and imaginary part $-x$ (dashed line) of the surface impedance of $CePd_3$ at low temperature. The absorptivity A is related to r according to $A\sim 4r$. The real part r was obtained by smoothing the experimental absorptivity data. The imaginary part was obtained from a Kramers-Kronig analysis of the data as explained in the text.

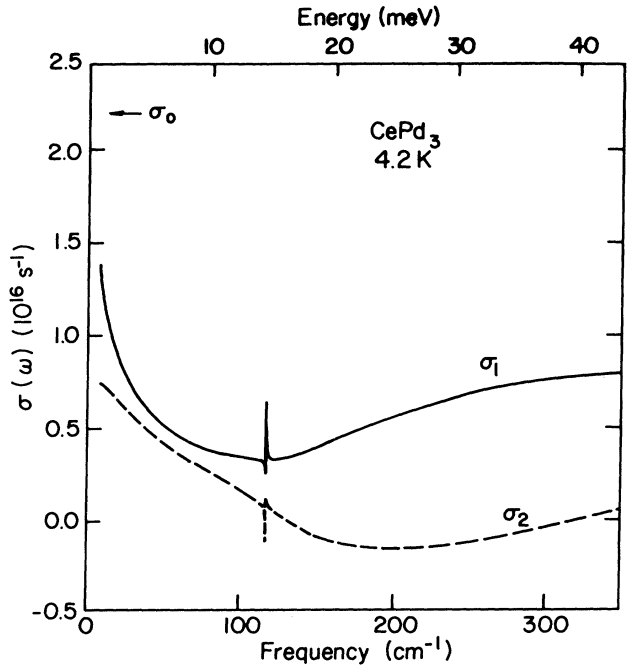

FIG. 10. Real (solid line) and imaginary (dashed line) parts of the optical conductivity of $CePd_3$ at low temperature. These curves were obtained from a Kramers-Kronig analysis of the absorptivity data as explained in the text. Note the minimum in σ_1 near 15 meV.

and imaginary parts of the surface impedance $r+ix$ and the ac conductivity $\sigma_1+i\sigma_2$. Note that $\sigma_1(\omega)$ is characterized by a *minimum*.

It is interesting to compare our low-temperature results with the recent low-frequency measurements of Hillebrands *et al.* on $CePd_3$ at room temperature.[30] From careful measurements of the reflectivity they deduced a slight increase in the ac conductivity of $CePd_3$ above its dc value with a peak at about 16 meV. Note that this change in conductivity from dc has the opposite sign to our results at 4 K, shown in Fig. 10.

Neutron scattering provides an alternative technique for investigating VF materials at meV energies. Unlike optical absorption, which is sensitive to charge excitations, neutron scattering is sensitive to spin excitations. In elastic neutron scattering experiments on $CePd_3$ Holland-Moritz *et al.*[60] reported a temperature-independent quasielastic peak with a $4f$ form factor and a width of 19 meV. There is no corresponding structure in the optical data. Likewise, there is no inelastic peak in the neutron data at 20 meV corresponding to the optical anomaly. The neutron scattering measurements only went down to 100 K in temperature, however, which is just where the optical anomaly washes out, hence the latter is not really a valid comparison. They find no evidence of crystal fields in $CePd_3$. Neutron scattering in $CePd_3$ is currently an active area of investigation, as Sec. III A 2 below will show.

2. *Optic phonons*

We turn our attention now to the sharp features O_1 and O_3 observed in etched $CePd_3$ at 14.7 and 21.6 meV. The feature O_1 at 118 cm^{-1} (14.7 meV) may be the sharpest feature ever seen in a metal. Figure 11 shows a detailed view of data in which O_1 has been fully resolved, taken on etched $CePd_3$ at helium temperature with resolution of 0.35 cm^{-1} (0.043 meV). The spike is very sharp, with a full width of about 3 cm^{-1} (0.4 meV), and it is nearly antisymmetric. The absorptivity drop from the maximum to the minimum occurs in a frequency interval of about 1.2 cm^{-1} (0.15 meV). The temperature dependence can be seen in Fig. 5 (in which O_1 is not fully resolved). As the temperature increases, the magnitude decreases, but it is still evident at temperatures as high as 100 K. The position and width of O_1 do not change appreciably as a function of temperature, which means that *at all temperatures above 4.2 K the width is less than kT*. Furthermore, there is no observable change in the position, width, or depth of the absorption line as a function of applied magnetic field up to a field of 75 kG. If it is assumed that the energy ΔE of the hypothetical magnetic transition depends linearly on the applied field H, i.e.,

$$\Delta E = g\mu_B H\ , \tag{10}$$

then the upper limit on the g value is $g \lesssim 0.07$ (a typical g value of, for example, $g=2$ would given an energy shift of 7 cm^{-1} at 75 kG). This rules out electronic transitions between sharp f-electron crystal -field levels, for example, as a possible origin, since such levels should split in an applied magnetic field.

The existence of such sharp structure in a metal is surprising, since the conduction electrons are expected to smear out such features. One set of excitations with well-defined energies, however, are the optic phonon modes at the center of the Brillouin zone. Because the incident photons interact with the phonons at $q=0$, where the optic modes are nearly dispersionless, these excitations can

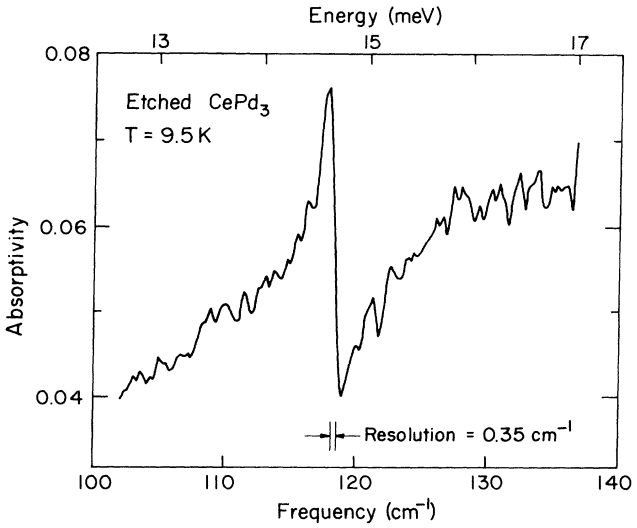

FIG. 11. Expanded view of the absorptivity of etched $CePd_3$ in the vicinity of the sharp spike O_1. The instrument resolution of 0.35 cm^{-1} (0.043 meV) is indicated on the figure. The drop from maximum to minimum absorptivity occurs in a frequency interval of about 1.2 cm^{-1} (0.15 meV).

be quite sharp. Furthermore, the optic phonon energies remain sharp even at room temperature.

Recently the room-temperature dispersion curves of $CePd_3$ have been measured with the use of neutron diffraction.[61] At $q=0$ three optic phonon modes have been observed at energies of 13.4, 15.9, and 21.2 meV. The symmetries of these modes are, respectively, Γ_4^-, Γ_5^-, and Γ_4^-. The Γ_5^- mode at 15.9 meV is not infrared active. The lowest and highest energy infrared active phonon modes are in good agreement with the energies of our optical spikes, O_1 and O_3 (hence the choice of labels). The close correspondence of the optical spikes with the neutron scattering data allows us to unambiguously identify the spikes as the $q=0$ optic phonon excitations. The slight difference between the energies observed by low-temperature optical measurements (14.7 and 21.6 meV) and the room-temperature neutron scattering (13.4 and 21.2 meV) may be due to a slight stiffening of the lattice at low temperature.

The phonon dispersion curves of the isostructural compounds YPd_3 and $DyPd_3$ should be quite similar to that of $CePd_3$. The observation of optic phonon excitations in the optical spectrum of $CePd_3$ thus suggests that analogous features should be present in YPd_3 and $DyPd_3$ at similar energies. No such features can be seen in either YPd_3 or $DyPd_3$, however, even in the high-resolution data for Ypd_3 shown in Fig. 2.

B. $YbCu_2Si_2$

The dc electrical resistivity of $YbCu_2Si_2$ has an anomalous temperature dependence similar to that of $CePd_3$, as shown in Fig. 12. The resistivity bends over toward saturation with increasing temperature, but unlike $CePd_3$ it does not reach maximum below room temperature. When the resistivity of isostructural nonmagnetic $LuCu_2Si_2$ is subtracted to obtain the anomalous component, however, a maximum is found at about 190 K (16 meV). The resistivity of $LuCu_2Si_2$ shows normal metallic behavior.

Quantitative absorptivity data unfortunately could not be obtained for $LuCu_2Si_2$ because of poor sample quality for optical measurements. The sample formed a fibrous or dendritic structure with many small vacuoles, which defeated our attempts to polish the sample to a smooth surface. A qualitative examination, however, indicates that there are no anomalies in the frequency dependence of $LuCu_2Si_2$.

The absorptivity of $YbCu_2Si_2$, shown in Fig. 13, has a qualitative behavior very similar to that seen in $CePd_3$ as a function of frequency and temperature. The absorptivity at helium temperature rises to a maximum near 220 cm^{-1}

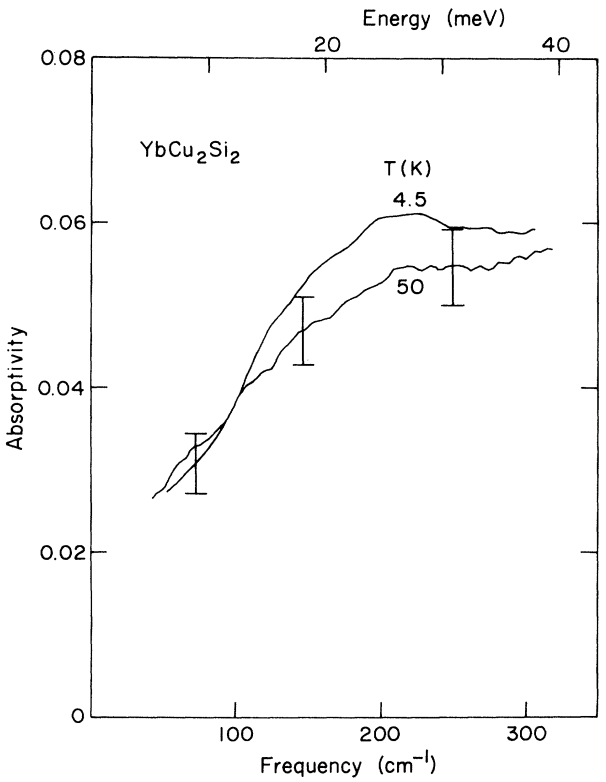

FIG. 13. Absorptivity of $YbCu_2Si_2$ as a function of frequency and temperature. The instrumental resolution is 8 cm^{-1}.

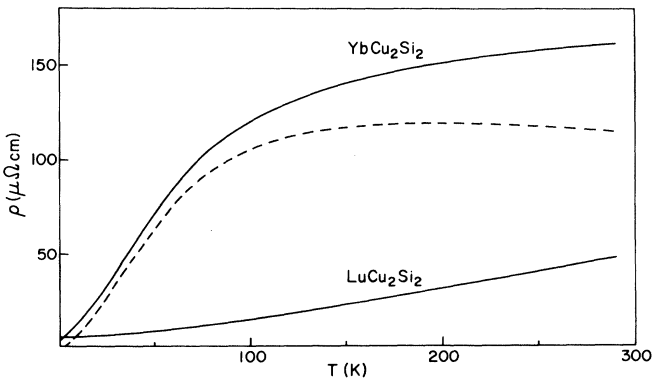

FIG. 12. Electrical resistivity of $YbCu_2Si_2$ and the isostructural compound $LuCu_2Si_2$. The dashed curve is obtained by subtracting the resistivity of $LuCu_2Si_2$ from that of $YbCu_2Si_2$.

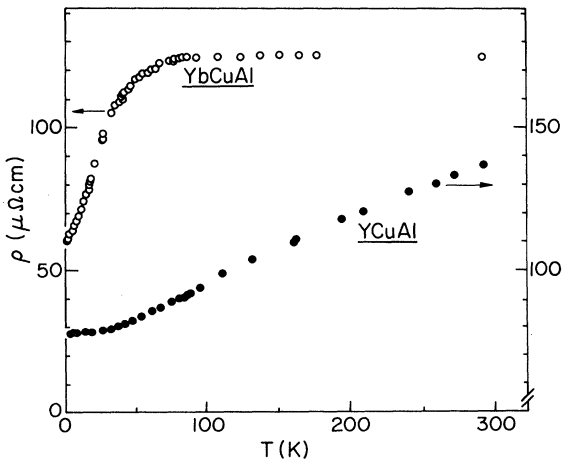

FIG. 14. Electrical resistivity of YbCuAl and the isostructural compound YCuAl. Note the difference in scales. (From W. C. M. Mattens, Ref. 70.)

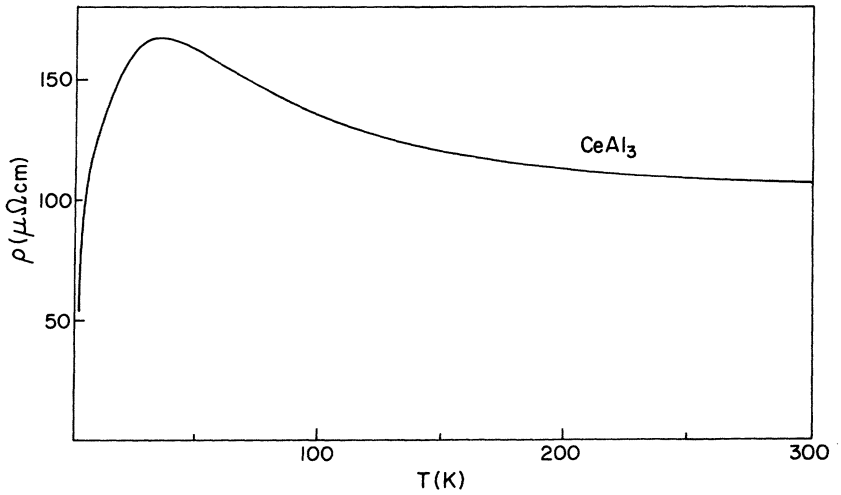

FIG. 15. Electrical resistivity of $CeAl_3$.

(27 meV), above which it remains roughly constant up to 310 cm^{-1} (38 meV). As a function of temperature the anomaly decreases in magnitude at least up to 50 K. Although we have quantitative data only up to 50 K, earlier qualitative data indicates that this decrease continues up to 150 K, as in $CePd_3$. High-resolution (1.4-cm^{-1}) data were also taken on $YbCu_2Si_2$, but no sharp features corresponding to those in $CePd_3$ were seen.

C. YbCuAl, $CeAl_3$, and $CeCu_2Si_2$

Although YbCuAl, $CeAl_3$, and $CeCu_2Si_2$ are VF materials, no obvious anomalies are seen in the optical properties of these materials above 3 meV. The anomalies in the temperature dependence of the magnetic susceptibility and transport properties of these materials, however, occur at temperatures nearly an order of magnitude lower than in $CePd_3$ and $YbCu_2Si_2$, with characteristic energies in the neighborhood of 1—3 meV. This is demonstrated by the resistivity curves measured for these materials, shown in Figs. 14—16.

Since the characteristic energies of these compounds are an order of magnitude below those of $CePd_3$ and $YbCu_2Si_2$, the optical anomalies may be occurring at much lower frequency. For this reason helium-temperature samples of YbCuAl were measured at low frequencies (between 10 and 70 cm^{-1}) using a lamellar grating interferometer for the frequency analysis. The absorptivity of YbCuAl is shown in Fig. 17 and agrees to within the experimental error with the Drude prediction. The results of these low-frequency measurements are suspect below about 25 cm^{-1} (3 meV), however, since we can no longer be assured that the nonresonant condition is satisfied. Although the dc resistivity changes by a factor of 2 between 4.2 and 150 K, as shown in Fig. 14, there is only a slight temperature dependence in the absorptivity, rather than the expected 40% increase. Thus the temperature dependence of the absorptivity is quantitatively inconsistent with the expected Drude result.

We have also measured $CeCu_2Si_2$ at low frequency, as shown in Fig. 18. $CeCu_2Si_2$ lies substantially below the Drude prediction, and in fact is well fit by a Drude curve corresponding to a resistivity of 280 $\mu\Omega$ cm. The excess

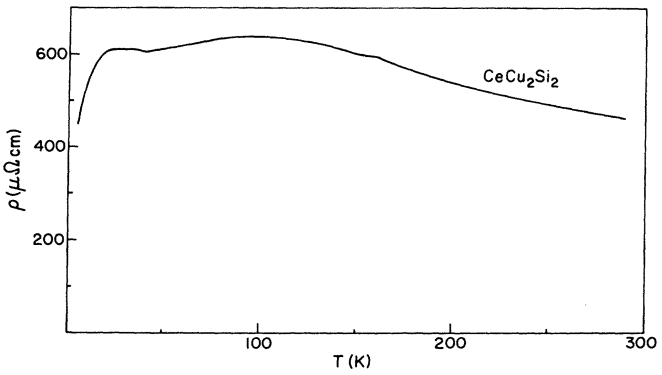

FIG. 16. Electrical resistivity of $CeCu_2Si_2$.

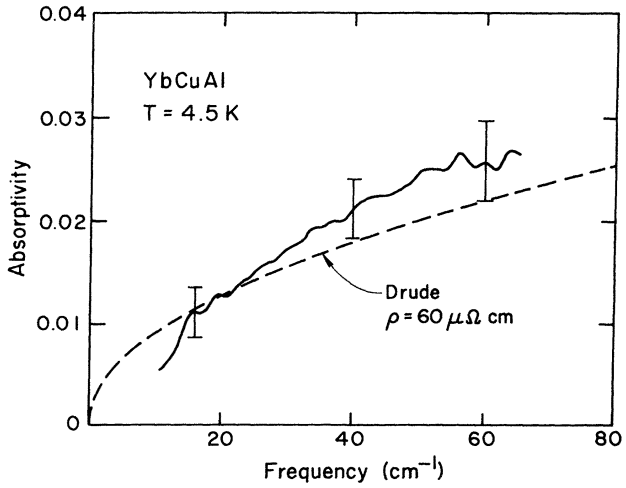

FIG. 17. Low-frequency absorptivity of YbCuAl at helium temperature. The dashed curve gives the predicted Drude response. The instrumental resolution is 2.2 cm^{-1}.

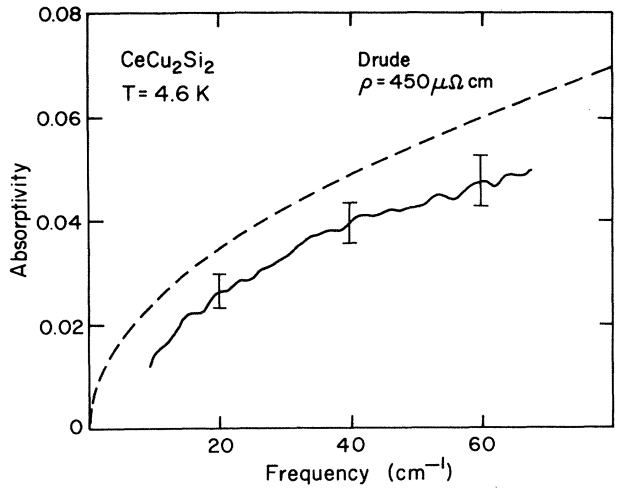

FIG. 18. Low-frequency absorptivity of $CeCu_2Si_2$ at helium temperature. The instrumental resolution is 2.2 cm^{-1}. The dashed curve is the predicted Drude absorptivity. The absorptivity of $CeCu_2Si_2$ has a Drude-type frequency dependence, but lies considerably below the Drude response calculated from the dc resistivity.

resistivity could arise from cracks in the sample, since changes in resistivity $CeCu_2Si_2$ with thermal cycling have been reported.[62] However, the resistivity of this sample $CeCu_2Si_2$ did reproduce to within 1% on each of three thermal cyclings, indicating that sample cracking may not be a problem here. The lack of correspondence between the measured absorptivity and dc resistivity of both $CeCu_2Si_2$ and YbCuAl may indicate optical structure at frequencies below 3 meV.

IV. CONCLUSION

Our experimental results are summarized in Table II, where we give the center frequency of the broad absorptivity anomaly for $CePd_3$ and $YbCu_2Si_2$ at helium temperature. This structure in the dielectric response of $CePd_3$ and $YbCu_2Si_2$ occurs at an energy comparable to the characteristic temperature kT_χ inferred from the temperature dependence of the magnetic susceptibility χ and to the temperature kT_ρ of the maximum in the dc electrical resistivity. The VF compounds YbCuAl, $CeAl_3$, and $CeCu_2Si_2$ do not show any obvious anomalies above 3 meV. Inspection of Table II, however, shows that the characteristic energies in these compounds are an order of magnitude lower than those of $CePd_3$ and $YbCu_2Si_2$. The absence of a resonance above 3 meV is thus not unexpected. The absorptivities of the integral valent-analog compounds YPd_3, $DyPd_3$, and $LuCu_2Si_2$ all have a Drude-type frequency dependence, even when a magnetic moment is present as in $DyPd_3$. In the one case where a quantitative comparison with Drude theory is possible (YPd_3) the agreement is good.

The two sharp features at 14.7 and 21.6 meV superimposed on the broad absorption anomaly in $CePd_3$ are clearly identified as the infrared-active optic phonon modes at zone center. A third mode seen in neutron scattering[61] is not infrared active. These features remain sharp even at elevated temperatures, where the thermal energy kT exceeds the linewidth by more than an order of magnitude.

In the Introduction we pointed out that departures from Drude behavior have also been observed in the intraband optical response of SmB_6 and TmSe. These two materials, however, are qualitatively quite different from the Ce and Yb intermetallics such as $CePd_3$ and $YbCu_2Si_2$: In the Sm and Tm compounds the *only* conduction electrons are those liberated from the $4f$ shell by the valence mixing. This difference shows up most dramatically in the dc conductivity, which is more typical of a semiconductor than a metal. In SmB_6 the conductivity *decreases* by as much as 4 orders of magnitude (for good samples) as the tempera-

TABLE II. Summary of the experimental results on valence-fluctuation systems. The second column gives the center frequency of the absorption anomaly at 4 K. The characteristic energies for these materials deduced from the magnetic susceptibility (kT_χ) and the dc resistivity (kT_ρ) are also listed.

Compound	Center frequency (meV)	kT_χ (meV)	kT_ρ (meV)
$CePd_3$ (polished)	20	25[a]	11[b]
$CePd_3$ (etched)	20	25[a]	11[b]
$YbCu_2Si_2$	27	9—24[c,d]	16[e,b]
$CeAl_3$	No resonance above 4 meV	1[f]	3[b]
$CeCu_2Si_2$	No resonance above 3 meV	1[g]	3[b]
YbCuAl	No resonance above 3 meV	3[h]	7[i,j]

[a]Reference 67.
[b]This work.
[c]$YbCu_2Si_2$ is anisotropic.
[d]Reference 11.
[e]Corrected for the resistivity of isostructural nonmagnetic $LuCu_2Si_2$.
[f]Reference 68.
[g]Reference 10.
[h]Reference 69.
[i]Taken as the temperature where the resistivity becomes constant.
[j]Reference 70.

ture drops from 300 to 4 K.[32] In the optical conductivity this appears as about an order of magnitude drop in $\sigma_1(\omega)$ between 80 meV and dc in SmB_6 thin films at 4 K (Ref. 32) (and, by extrapolation to the dc conductivity, a 4 order of magnitude drop in single crystals). This is cited as evidence for a deep minimum, possibly even a small bandgap, in the density of states at the Fermi energy in SmB_6.[32] This optical behavior is quite distinct from that observed in $CePd_3$. The conductivity of TmSe likewise decreases by about an order of magnitude in a semiconductorlike fashion between room temperature and 4 K.[28] The optical response of TmSe,[28] though, is qualitatively similar to that of $CePd_3$ and $YbCu_2Si_2$. At room temperature the optical conductivity rises *above* the dc value when the photon energy falls below about 0.2 eV. When the sample is cooled to 77 K the reflectivity *decreases,* indicating an *increase* in the absorptivity apparently above the Drude prediction. This behavior is in fact qualitatively attributed by the investigator to conduction-electron scattering from an f level at the Fermi level.[28] In view of the qualitative differences between TmSe and the Ce and Yb intermetallics, however, the mechanism responsible for the optical response of the two classes of materials may be quite different.

The broad absorptivity enhancement observed in $CePd_3$ and $YbCu_2Si_2$ arises solely as a consequence of the VF nature of these materials. We attribute the additional absorption to the frequency-dependent scattering of conduction electrons presumably from a resonant level located near the Fermi level.

ACKNOWLEDGMENTS

We wish to thank Ted Mihalisin and Willem Mattens for providing two of the samples used in this work. We also thank Jim Allen for providing us with his room-temperature reflectivity data on $CePd_3$ used in the Kramers-Kronig analysis, and Constantine Stassis for his unpublished neutron scattering data which made identification of the $CePd_3$ optic phonon modes possible. We profited from valuable discussions with both. The research at Cornell University was supported by the National Science Foundation under Grant No. DMR-81-06097, Cornell University Materials Science Center Report No. 5073. The research at the University of California, San Diego, was supported by the U.S. Department of Energy under Contract No. DE-AT03-76ER70227.

---

*Present address: General Motors Research Laboratory, 12 Mile and Mound Road, Warren, MI 48090.

†Present address: Solid State Division, Oak Ridge National Laboratory, P.O. Box X, Oak Ridge, TN 37830.

[1]For reviews, see Refs. 2–8.

[2]J. M. Lawrence, P. S. Riseborough, and R. D. Parks, Rep. Prog. Phys. 44, 1 (1981).

[3]M. B. Maple, L. E. Delong, and B. C. Sales, in *Handbook on the Physics and Chemistry of Rare Earths,* edited by K. A. Gschneider and L. Eyring (North-Holland, Amsterdam, 1978), Vol. I, pp. 797–846.

[4]*Proceedings of the International Conference on Valence Instabilities and Related Narrow-Band Phenomena,* edited by R. D. Parks (Plenum, New York, 1977).

[5]*Proceedings of the International Conference on Valence Fluctuations in Solids,* edited by L. M. Falicov, W. Hanke, and M. B. Maple (North-Holland, Amsterdam, 1981).

[6]M. Campagna, G. K. Wertheim, and E. Bucher, in *Spectroscopy of Homogeneous Mixed Valence Rare Earth Compounds,* Vol. 30 of *Structure and Bonding,* edited by J. D. Dunitz, P. Hemmerich, J. A. Ibers, C. K. Jorgensen, J. B. Neilands, D. Reinen, and R. J. P. Williams (Springer-Verlag, New York, 1976), p. 99.

[7]J. H. Jefferson and K. W. H. Stevens, J. Phys. C 11, 3919 (1978).

[8]C. M. Varma, Rev. Mod. Phys. 48, 219 (1976).

[9]W. E. Gardner, J. Penfold, T. F. Smith, and I. R. Harris, J. Phys. F 2, 133 (1972).

[10]B. C. Sales and R. Viswanathan, J. Low Temp. Phys. 23, 449 (1976).

[11]B. C. Sales and D. K. Wohlleben, Phys. Rev. Lett. 35, 1240 (1975).

[12]P Scoboria, J. E. Crow, and T. Mihalisin, J. Appl. Phys. 50, 1895 (1979).

[13]G. Güntherodt and F. Holtzberg, Solid State Commun. 18, 181 (1976).

[14]E. Kaldis and P. Wachter, Solid State Commun. 11, 907 (1972).

[15]J. L. Kirk, K. Vedam, V. Narayanamurti, A. Jayaraman, and E. Bucher, Phys. Rev. B 6, 3023 (1972).

[16]D. W. Pohl, R. Jaggi, K. Gisler, and H. Weibel, Solid State Commun. 17, 705 (1975).

[17]D. W. Pohl, Phys. Rev. B 15, 3855 (1977).

[18]I. A. Smirnov, R. Suryanarayanan, and S. G. Shul'man, Phys. Status Solidi B 73, K137 (1976).

[19]I. A. Smirnov, R. Suryanarayanan, and S. G. Shul'man, Phys. Status Soildi B 75, K153 (1976).

[20]T. I. Volkonskaya, A. I. Shelykh, T. L. Bzhalava, S. G. Shul'man, T. B. Zukova, and I. A. Smirnov, Fiz. Tverd. Tela (Leningrad) 17, 1172 (1975) [Sov. Phys.—Solid State 17, 751 (1975)].

[21]J. W. Allen, in *Valence Instabilities and Related Narrow-Band Phenomena,* edited by R. D. Parks (Plenum, New York, 1977), p. 533–535.

[22]B. Batlogg, E. Kaldis, A. Schlegel, and P. Wachter, Phys. Rev. B 14, 5503 (1976).

[23]B. Batlogg, A. Schlegel, and P. Wachter, Physica B&C 86-88, 229 (1977).

[24]A. Schlegel, E. Kaldis, P. Wachter, and Ch. Zürcher, Phys. Lett. A66, 125 (1978).

[25]B. Batlogg, E. Kaldis, A. Schlegel, and P. Wachter, Phys. Lett. A56, 122 (1976).

[26]B. Batlogg, Phys. Rev. B 23, 650 (1981).

[27]G. Güntherodt, R. Keller, P. Grunberg, A. Frey, W. Kress, R. Merlin, W. B. Holzapfel, and F. Holtzberg, in *Proceedings of the International Conference on Valence Instabilities and Related Narrow-Band Phenomena,* Ref. 4, pp. 321–334.

[28]B. Batlogg, Phys. Rev. 23, 1827 (1981).

[29]J. W. Allen, R. J. Nemanich, and S.-J. Oh, J. Appl. Phys. 53, 2145 (1982).

[30]B. Hillebrands, G. Güntherodt, R. Pott, W. König, and A. Breitschwerdt, Solid State Commun. 43, 891 (1982).
[31]J. W. Allen, R. M. Martin, B. Batlogg, and P. Wachter, J. Appl. Phys. 49, 2078 (1978).
[32]B. Batlogg, P. H. Schmidt, and J. M. Rowell, in *Proceedings of the International Conference on Valence Fluctuations in Solids,* Ref. 5, pp. 267–269.
[33]B. P. Clayman, R. W. Ward, and J. P. Tidman, Phys. Rev. B 16, 3734 (1977).
[34]M. I. Nathan, F. Holtzberg, J. E. Smith, Jr., J. B. Torrance, and J. C. Tsang, Phys. Rev. Lett. 34, 467 (1975).
[35]G. Güntherodt, R. Merlin, A. Frey, and M. Cardona, Solid State Commun. 27, 551 (1978).
[36]G. Güntherodt, A. Jayaraman, W. Kress, and H. Bilz, Phys. Lett. 82A, 26 (1981).
[37]H. Boppart, A. Treindl, and P. Wachter, in *Proceedings of the International Conference on Valence Fluctuations in Solids,* Ref. 5, pp. 103–111.
[38]F. E. Pinkerton, A. J. Sievers, J. W. Wilkins, M. B. Maple, and B. C. Sales, Phys. Rev. Lett. 47, 1018 (1981).
[39]F. E. Pinkerton, A. J. Sievers, J. W. Wilkins, M. B. Maple, and B. C. Sales, in *Valence Fluctuations in Solids,* edited by L. M. Falicov, W. Hanke, and M. B. Maple (North-Holland, New York, 1981), p. 177.
[40]The sample of YbCuAl was generously provided by Dr. Willem Mattens of the Universiteit van Amsterdam, Amsterdam, The Netherlands.
[41]The sample $CePd_3$(a) was made by one of us (B.S.), while the samle $CePd_3$(b) was provided by Professor Theodore Mihalisin of Temple University, Philadelphia, Pennsylvania.
[42]P. O. Nilsson, in *Solid State Physics,* edited by H. Ehrenreich, F. Seitz, and D. Turnbull (Academic, New York, 1974), Vol. 29, p. 139.
[43]L. D. Landau and E. M. Lifshitz, *Electrodynamics of Continuous Media* (Pergamon, Oxford, 1960), p. 279–284.
[44]F. Wooten, *Optical Properties of Solids* (Academic, New York, 1972).
[45]R. W. Ward, Infrared Phys. 16, 385 (1976).
[46]P. L. Richards and M. Tinkham, Phys. Rev. 119, 575 (1960).
[47]F. E. Pinkerton and A. J. Sievers, Infrared Phys. 22, 377 (1982).
[48]J. D. Leslie and D. M. Ginsberg, Phys. Rev. 133, A362 (1964).
[49]D. B. Tanner and A. J. Sievers, Phys. Rev. B 8, 1978 (1973).
[50]B. Farnsworth and T. Timusk, Phys. Rev. B 10, 2799 (1974).
[51]R. W. Ward and B. P. Clayman, Solid State Commun. 17, 1297 (1975).
[52]B. P. Clayman, R. W. Ward, and J. P. Tidman, Phys. Rev. B 16, 3734 (1977).
[53]D. R. Karecki and B. P. Clayman, Phys. Rev. B 19, 6367 (1979).
[54]W. E. Lamb, Jr., Phys. Rev. 70, 308 (1946).
[55]K. C. Johnson, Ph.D. Thesis, Cornell University, 1972.
[56]D. B. Tanner, Ph.D. Thesis, Cornell University, 1972.
[57]A. J. Sievers, Opt. Soc. Am. 68, 1505 (1978).
[58]R. L. Blewitt, Ph.D. Thesis, Cornell University, 1973.
[59]T. Mihalisin (private communication).
[60]E. Holland-Moritz, M. Loewenhaupt, W. Schmatz, and D. K. Wohlleben, Phys. Rev. Lett. 38, 983 (1977).
[61]We are grateful to C. Stassis for sending us his unpublished data.
[62]W. Franz, A. Griessel, F. Steglich, and D. Wohlleben, Z. Phys. B 31, 7 (1978).
[63]I. R. Harris and M. Norman, J. Less-Common Metals 15, 285 (1968).
[64]W. Rieger and E. Parthé, Monatesh. Chem. 100, 444 (1969).
[65]J. H. N. van Vucht and K. H. J. Buschow, J. Less-Common Metals 10, 98 (1965).
[66]H. Oesterreicher, J. Less-Common Metals 30, 225 (1973).
[67]B. C. Sales, J. Low Temp. 28, 107 (1977).
[68]K. H. J. Buschow and J. F. Fast, Z. Phys. Chem. N.F. 50, 1 (1966).
[69]W. C. M. Mattens, R. A. Elenbaas, and F. R. de Boer, Commun. Phys. 2, 147 (1977).
[70]W. C. M. Mattens (unpublished).